DINAME 2017 - Proceedings of the XVII International Symposium on Dynamic Problems of Mechanics
A. T. Fleury, D. A. Rade, P. R. G. Kurka (Editors), ABCM, São Sebastião, SP, Brazil, March 5-10, 2017

DINAME 2017 – Structural Characterization of the Block and Stator Group of a Hermetic Compressor

Jean Carlos Marcon[1], Arcanjo Lenzi[1], Olavo Messias Silva[1], Walter dos Santos Sousa[1]

[1] Federal University of Santa Catarina – UFSC, Campus Trindade, jean.marcon@lva.ufsc.br, arcanjo@lva.ufsc.br, olavo@lva.ufsc.br, walter.sousa@lva.ufsc.br

Abstract: The vibroacoustic analysis of structures and equipment has become important due to the search for reliability, energy efficiency and comfort in product development. In homes, sound quality is directly dependent on devices that produce low noise levels. Hermetic compressors present in these environments are important noise sources that require design studies and changes to minimize radiated noise. In this context, the Finite Element Method (FEM) provides satisfactory computational representations that allow the study of these products at a reduced cost. Considering that one of the main sources of the vibration and noise of a hermetic compressor is the block and stator group, which supports the entire load during the cyclical process of refrigerant gas compression, this paper presents the application of the FEM to the characterization of these components. The block was partitioned into three regions for the fitting of the different isotropic properties. In the case of the laminated stator, the homogenization method was applied for the determination of equivalent orthotropic properties for the volume of the blades and the boundary conditions provided by bolted joints. Obtaining a set of physical properties is based on the minimization of the residuals between the numerical and experimental natural frequencies in the frequency range of 0-10 kHz. Therefore, we used the multi-objective genetic algorithm method (MOGA) together with commercial software Ansys®. The technique that considers the block division into different isotropic regions provided better results than considering a uniform piece, confirming its efficacy in the computational representation of components that have geometric constraints and variations in the microstructural properties arising from the manufacturing process. The simplified model of the stator obtained by the method of homogenization showed satisfactory experimental correlation. By applying the boundary conditions between the block and the stator a simplified group model was obtained and validated experimentally. Finally, the group model enables the realization of advanced studies for the purpose of promoting vibroacoustic improvements.

Keywords: Finite element method, model updating, hermetic compressor.

INTRODUCTION

The hermetic compressor, the main component of a cooling system, is a major source of noise, being responsible for the excitation of the entire system. The alternative type is the most commonly used in small refrigeration systems, such as refrigerators, freezers and air conditioners (Doi, 2011; Fulco, 2014; Fontanela *et al.*, 2016.). The process consists of pumping refrigerant through the refrigeration circuit, in which the compression is performed by the linear reciprocating displacement of a piston.

All of the internal compressor assembly is attached to the housing by a discharge tube and is supported by springs fixed to the bottom of the stator, as shown in Fig. 1a. According to Fig. 1b, the block has four bases attached to the stator to provide mutual exchange of vibrational energy. Similarly, its two bearings are connected to the rotating shaft, through which forces are transmitted (Fulco, 2014). The torque generated by the electric motor, together with the rotor inertia effects, provides the compression of the refrigerant in the cylinder.

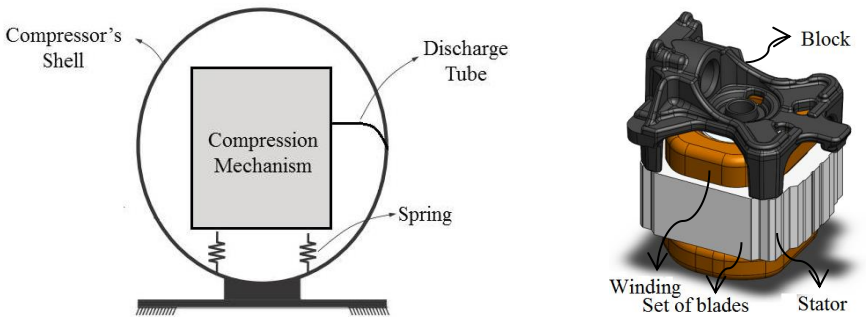

Figure 1 – a) Representation of the electric motor. b) Block coupled with the stator.

The final noise radiator to the external environment is the compressor shell (Fontanela *et al.* 2016), whose excitation comes from the internal group of components. It has been noted that the block and stator group are key to the analysis and control of vibration and noise from the compressor. For this reason, they are objects of study in this work.

Therefore, the fitting of the model for the block and stator set of the electric motor was carried out based on experimental results. The individual validated block and stator models are the basis of the coupled set model.

Correlation methods

Correlation methods applied to the model fitting take into account a comparison between the natural frequencies obtained from numerical and experimental frequency response functions (FRFs) (Mothershead and Friswell, 1993). For a comparison of the "p" pairs of numeric natural frequencies "ω_p^N" and experimental frequencies "ω_p^E" a percentage relative difference can be quantitatively adopted, as given by Eq. (1).

$$\Delta\omega_n\left(\omega_p^N, \omega_p^E\right) = \frac{\omega_p^N - \omega_p^E}{\omega_p^E} \tag{1}$$

Another common way to correlate natural frequencies is to calculate the average deviation "$\overline{\Delta\omega_n}$", given by the simple average of the module of the individual deviations of the natural frequency pairs "p", as shown in Eq. (2):

$$\overline{\Delta\omega_n} = \frac{1}{N_p}\sum_{p=1}^{N_p}\left|\Delta\omega_n\left(\omega_p^N, \omega_p^E\right)\right| \tag{2}$$

In addition, Allemagne Brown (1982) recommend calculating an overall divergence between the pairs of natural frequencies, as indicated in Eq. (3):

$$\ell_\omega = \sqrt{\sum_{p=1}^{N}\frac{(\omega_p^N - \omega_p^E)^2}{(\omega_p^E)^2}} \tag{3}$$

The comparison between numerical and experimental FRFs also provides information on the representativeness of the fitted models. Thus, this will also be adopted as an evaluation criterion.

Iterative methods of updating models have been widely studied and applied to acoustic systems. They are based on minimizing a norm calculated from a "ℓ" residual. This residual is usually dependent on differences between pairs "p" of numerical quantities "N" and experimental quantities "E" which, in general, is associated with the total mass (Eq. 4) and the natural frequency (Eq. 5).

$$\ell_m = m^N - m^E \tag{4}$$

$$\{\ell_{\omega_p}\} = \frac{\omega_p^N - \omega_p^E}{\omega_p^E} \tag{5}$$

In the model fitting process, the residuals of the natural frequencies are minimized through the use of a Multi-Objective Genetic Algorithm (MOGA), the input parameters being the physical properties of the component material, such as the modulus of elasticity and the Poisson coefficient.

BLOCK

For the calibration of the block model, an experimental modal analysis was performed to obtain the modal parameters, highlighting natural frequencies, vibration modes and damping.

Experimental modal analysis of block

The experimental setup used in the tests is shown in Fig. 2a. The block was impacted at the point indicated in Fig. 2c using an impact hammer. The acceleration response signals were measured at the points shown in Fig. 2c along the three orthogonal axes employing a uniaxial accelerometer, as shown in Fig. 2b.

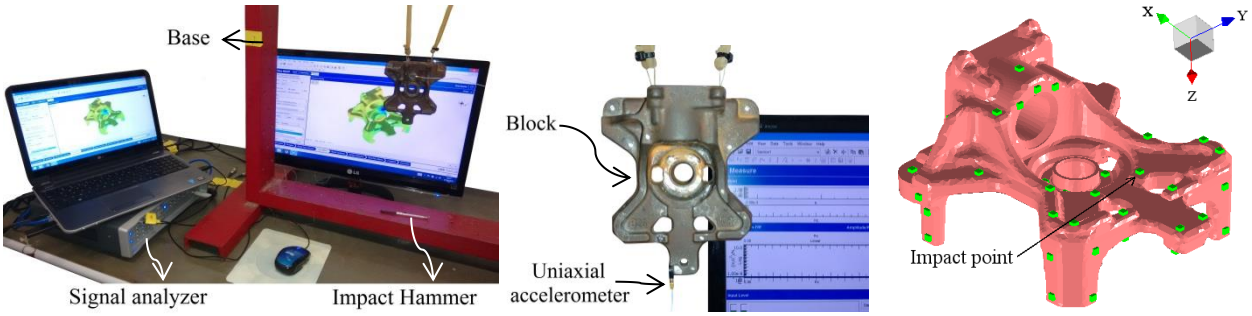

Figure 2 – a) Experimental setup for modal analysis of the block. b) Uniaxial accelerometer fixed on the block. c) Point of impact and experimental mesh.

The resulting FRFs were used to calculate the modal parameters of the system to calibrate the numerical finite element model.

Numerical model of block

By minimizing the residuals between the numerical and experimental natural frequencies with the aid of MOGA, two different numerical models were fitted. The first is shown in Fig. 3a and considers that the block is composed of homogeneous material with isotropic physical properties. In the second, the block is asymmetrically divided into three regions (Fig. 3b), in which different moduli of elasticity (E) were fitted, maintaining the same density and Poisson's ratio. In both, the quadratic tetrahedral finite element was used.

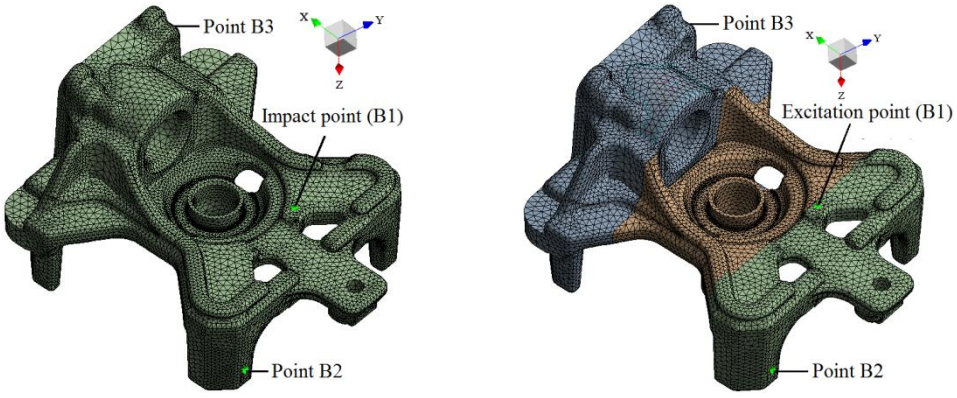

Figure 3 – a) Mesh for compressor block with geometry correction only. b) Mesh for partitioned block with geometry correction.

The comparison between the numerical and experimental natural frequencies are shown in Table 1. On evaluating the average relative error between the sixteen natural frequencies, the model of the partitioned block showed a better result (1.2%) compared to the uniform block (1.4%). The same applies to the overall differences between the natural frequencies of the two models (6.2% and 5.4%, respectively). The representativeness of the partitioned model considers greater sensitivity to manufacturing imperfections present in the real piece, with stiffness variations throughout its structure. It should be noted that the geometry of the block represented by the set of nodes is not perfect and this contributes to the imprecision of the model.

Table 1 – Comparison between the numerical and experimental results for the three models of the block: initial (absence of geometry correction), homogeneous with geometry correction and partitioned with geometry correction.

		Initial		Uniform		Partitioned	
Order	ω^E (Hz)	ω^N (Hz)	$\Delta\omega_n$ (%)	ω^N (Hz)	$\Delta\omega_n$ (%)	ω^N (Hz)	$\Delta\omega_n$ (%)
1	1531.0	1511.8	-1.3	1511.3	-1.3	1506.8	-1.6
2	2012.6	1996.6	-0.8	2050.6	1.9	2055.1	2.1
3	2464.9	2377.2	-3.6	2413.4	-2.1	2442.0	-0.9
4	3302.4	3602.8	9.1	3347.1	1.4	3299.9	-0.1
5	4100.7	4144.1	1.1	4196.1	2.3	4199.8	2.4
6	4297.4	4281.8	-0.4	4263.1	-0.8	4265.6	-0.7
7	4800.8	4731.8	-1.4	4737.3	-1.3	4757.0	-0.9
8	5306.4	5196.5	-2.1	5256.6	-0.9	5255.9	-1.0
9	5410.5	5390.9	-0.4	5320.7	-1.7	5340.1	-1.3
10	6518.3	6383.0	-2.1	6453.7	-1.0	6517.8	0.0
11	6921.1	6866.8	-0.8	6876.8	-0.6	6896.6	-0.4
12	7448.3	7547.3	1.3	7433.8	-0.2	7336.5	-1.5
13	7532.6	7637.1	1.4	7600.8	0.9	7610.2	1.0
14	8540.9	8800.2	3.0	8794.0	3.0	8707.7	2.0
15	9593.0	9617.1	0.3	9662.8	0.7	9653.3	0.6
16	9750.2	9918.1	1.7	9956.2	2.1	9950.9	2.1
Average:			1.9		1.4		1.2
ℓ_ω **(%):**			11.2		6.2		5.4

A constant loss factor "η" with the frequency was applied to the partitioned block. A comparison between numerical and experimental FRFs is shown in Figs. 4 and 5. The fitted numerical model is representative and lies within the region of experimental variability, which is based on the analysis of seven different pieces.

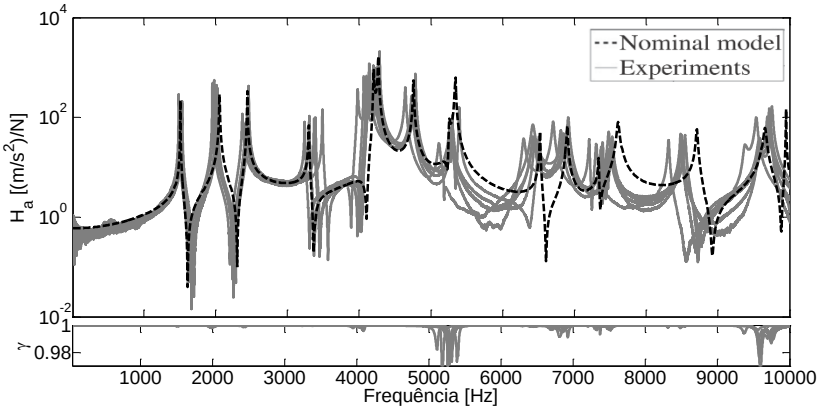

Figure 4 – Accelerance values obtained from the response measurement at point B2 (x direction) and excitation at point B1 (z direction).

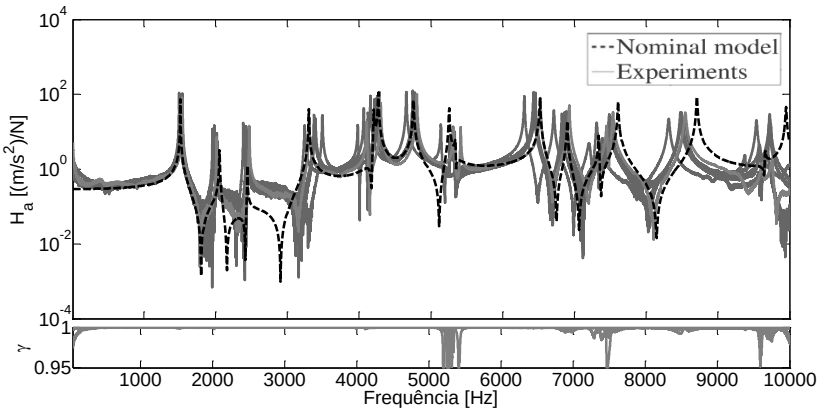

Figure 5 – Accelerance values obtained from the response measurement at point B3 (y direction) and excitation at point B1 (z direction).

The next component to be represented by finite elements is the stator, as shown below.

STATOR

This section describes the experimental modal analysis of the stator carried out to obtain the modal parameters and subsequently the fitting of the numerical model. As in the case of the block, the maximum frequency stipulated in the analysis was 10 kHz.

Experimental modal analysis of stator

The configuration used in the experimental modal analysis is shown in Figs. 6a and 6b. Figure 6a shows the shaker connection with the stator for the application of excitement using white noise in the radial direction of the piece. The connection is made through the stinger, the force signals are measured by the load cell and the acceleration signals are measured with triaxial accelerometers at 50 points, as indicated in Fig. 6c. A second transverse excitation was adopted as a reference, as shown in Fig. 6b. As in the case of the block, the stator is suspended by a support.

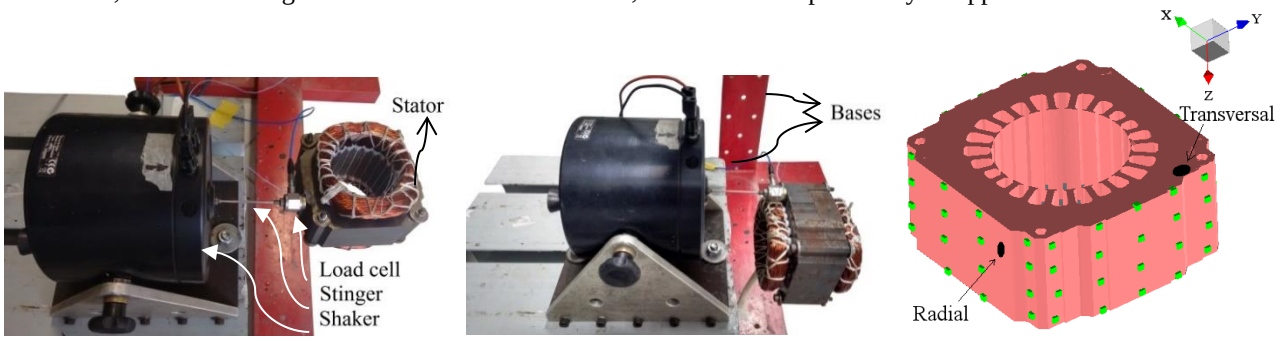

a) b) c)

Figure 6 – Experimental setup for modal analysis of the stator: a) excitation in the radial direction; b) excitation in the transversal direction; c) experimental mesh with 50 points.

The numerical model was fitted using the modal parameters obtained experimentally, as highlighted in the next section.

Numerical model of stator

To compose the complete model of stator, each of its pieces was modeled separately. The typical physical properties of the bolts and washers were standardized. In this case, both quadratic tetrahedral elements and quadratic hexahedral elements were adopted.

Through the method of homogenization (Kalamkarov, Andrianov and Danishevs'kyy, 2009; Millithaler, 2015; Millithaler et al., 2015), the blades were represented by two distinct homogeneous volumes, composed of elements of the quadratic hexahedral type: the first considers the region of the stator teeth and the second considers the region outside the teeth, as shown in Fig. 7b. In addition, the subsystems are coupled by contact interfaces, as shown in Fig. 7a, for the application of the modal synthesis methods (Craig and Bampton, 1968; Herting, 1985; Martinez *et. al.*, 1984; Fontanela *et al.*, 2016). On the surfaces in contact, between the washers and the stator blade pack, the friction effect was considered, whose formulation is non-linear. The contact interfaces between the screws and the washers allow them to be attached. Lastly, a typical pretension is applied to the screws to approximate the physical condition of the component.

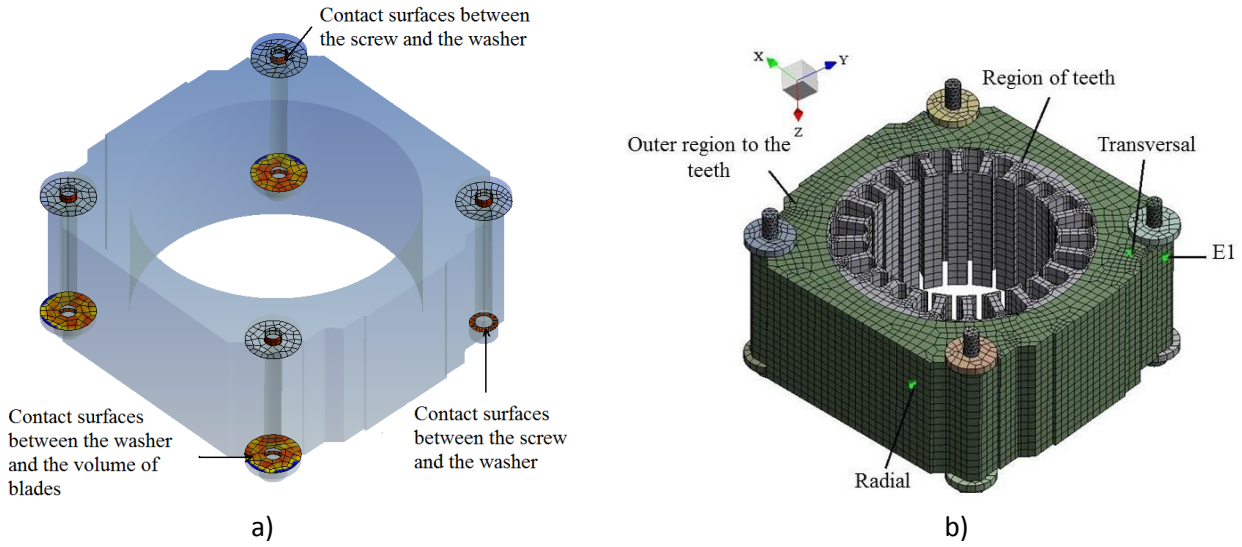

Figure 7 – a) Specification of the contact regions between the stator components. b) Numerical model of the simplified stator.

By means of the application of MOGA, the orthotropic properties were adjusted for the two regions of the blade pack, in order to minimize the residuals between 5 pairs of numerical and experimental natural frequencies. The comparative results are shown in Table 2. It can be observed that the average deviation between pairs of natural frequencies is 3.0% and the total is 8.6%, results that are considered satisfactory.

Table 2 – Correlation between the numerical and experimental natural frequencies for the stator model without the physical presence of the winding.

Order	ω^E (Hz)	ω^N (Hz)	$\Delta\omega_n$ (%)
1	1084.0	1136.9	4.9
2	1477.3	1489.8	0.8
3	3621.4	3656.5	1.0
4	3848.4	3796.2	-1.4
5	5129.3	4780.0	-6.8
Average			3.0
ℓ_ω (%):			8.6

A loss factor "η", which is constant with frequency, was applied to the blade pack. A comparison between the numerical and experimental FRFs is shown in Figs. 8 and 9.

The numerical model of the group is representative and is within the region of experimental variation obtained from a sample of seven distinct pieces. However, due to the absence of the winding representation, the simplified numerical model loses precision in the frequency range of 300 to 900 Hz. The model also shows low sensitivity at frequencies above 7 kHz, and these divergences may occur due to the lack of physical representation of the discontinuities of the laminated structure, when the homogenization method is used.

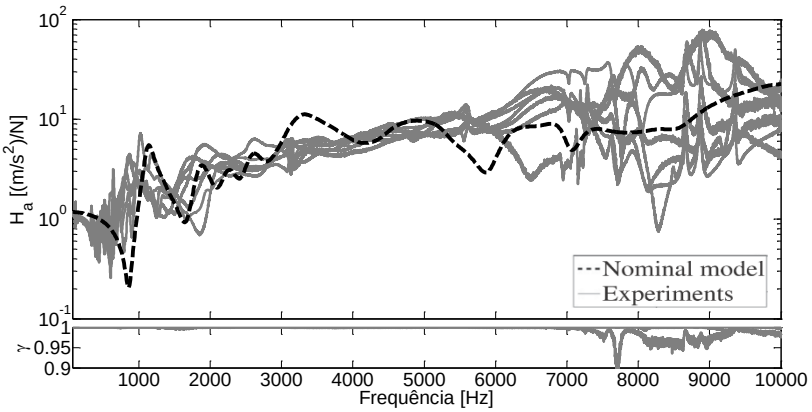

Figure 8 – Comparison between the numerical and experimental accelerance values for transversal excitation (z direction) and response measurement at point E1 (z direction).

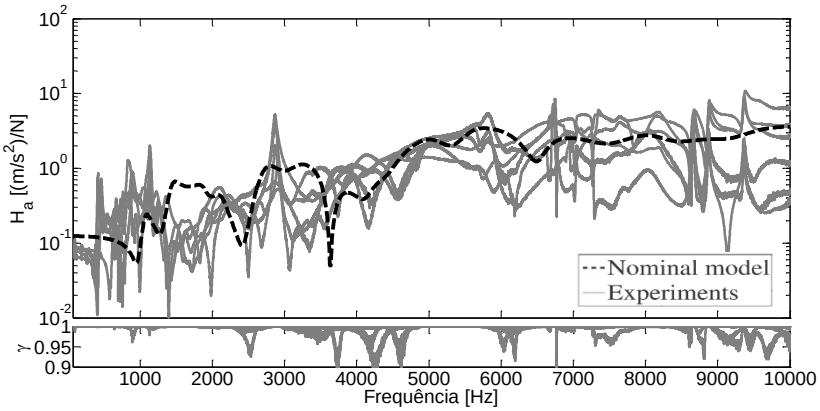

Figure 9 – Comparison between the numerical and experimental accelerance values for radial excitation (y direction) and response measurement at point E1 (z direction).

In the next section, the fitted models for the block and stator are coupled.

COUPLING BETWEEN THE BLOCK AND THE STATOR

Figure 10a shows the contact areas between the models for the block and the stator. In this case, the same properties specified for the individual models of components were maintained. The model for the set is shown in Fig. 10b. The effect of applying the typical pretension on the screws is shown in Fig. 10c (light blue).

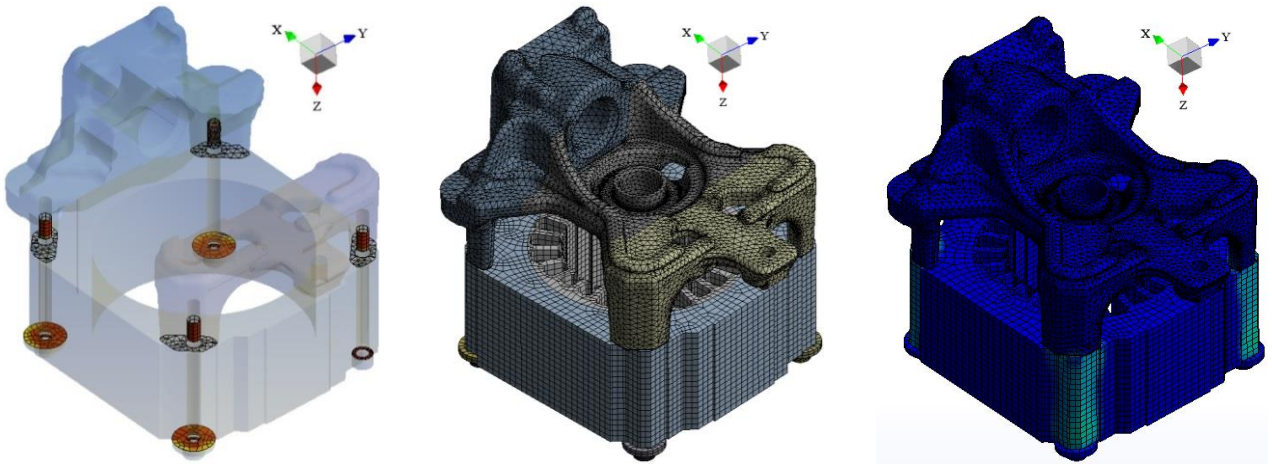

a) b) c)

Figure 10 – a) Representation of the contact zones between the components. b) Numerical mesh for block and stator group. c) Representation of the effect of pre-tension of the clamping components.

The set was excited by a shaker with a white noise signal, according to the configuration shown in Fig. 11a. The experimental apparatus is the same as that used in the stator test. Figure 11b shows the points at which the acceleration response (E1 and B2, in the x direction) was obtained. The excitation application point is shown in Fig. 11c (B4, in the x

direction). The same procedure was carried out for the numerically comparison of the FRFs, as shown in Figs. 12 and 13.

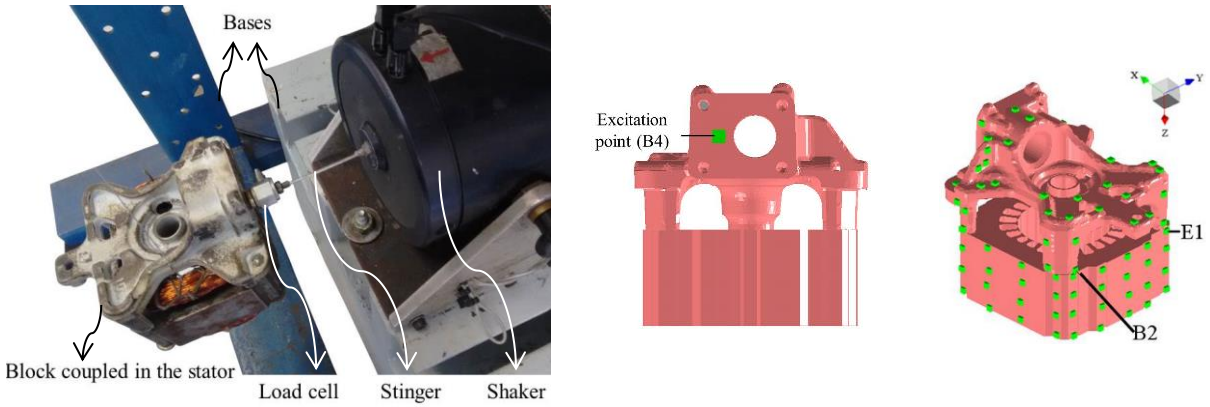

Figure 11 – a) Experimental test configuration. b) Indication of the reference measurement point (B4, in the x direction). c) Indication of the response measurement points (E1 and B2, in the x direction).

According to the data in Figs. 12 and 13, the numerical model for the group is representative and shows similar behavior to the set of three samples tested experimentally.

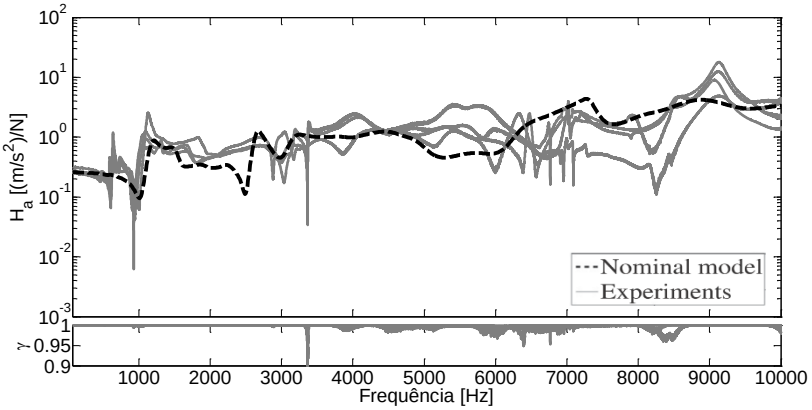

Figure 12 – Comparison between the numerical and experimental accelerance values for the excitation at point B4 (x direction) and response measurement at point B2 (x direction).

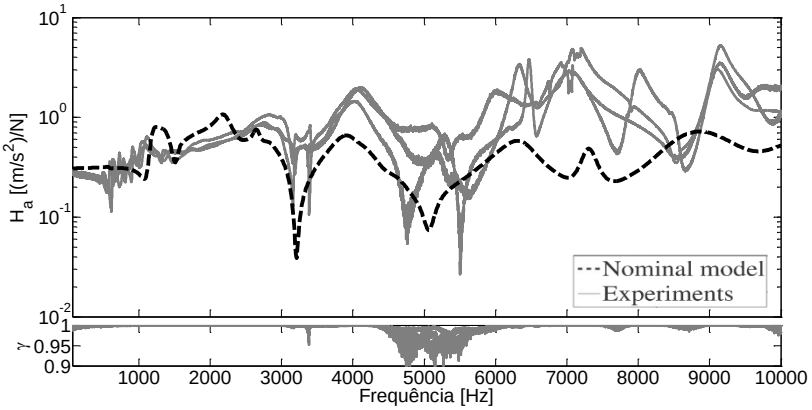

Figure 13 – Comparison between the numerical and experimental accelerance values for the excitation at point B4 (x direction) and response measurement at point B1 (x direction).

These results show that an improvement in the representativeness of this type of electromechanical structure was achieved at a relatively low computational cost, allowing more accurate vibroacoustic analysis of the components involved.

CONCLUSIONS

Satisfactory numerical representations of the block, stator and a coupling between the two components was obtained.

However, the simplified model presented does not show good accuracy between 300 and 900 Hz. The lack of sensitivity between the model and the real stator part was shown to have a greater influence from 7 kHz, mainly due to the lack of physical representation of the discontinuities of the blades, using the homogenization method. However, this had less influence in the case of the model for the block and stator set.

The division of the block into asymmetric regions for the fitting of the isotropic properties further minimized the residuals between the numerical and experimental natural frequencies, for which the average was 1.2%, reducing the limitations associated with the geometric representation and homogeneity of material. The homogenization method also provided good results in the numerical representation of the stator based on the fitting of the equivalent orthotropic properties, providing an average relative error of 3.0% between the reference numerical and experimental natural frequencies.

The modal synthesis performed with the aid of commercial software Ansys® was considered adequate and the simplified assembly model is representative, enabling computational vibroacoustic analysis.

ACKNOWLEDGMENTS

The authors are grateful to the company Embraco for technical support and permission to publish this work.

The first author received financial support from the Brazilian governmental agency CNPq, which is gratefully acknowledged.

REFERENCES

Allemang, R. J.; Brown, D. L., 1982, Correlation coefficient for modal vector analysis, Proceedings of the 1st International Modal Analysis Conference, Orlando: [s.n.]., p. 110-116.

Craig, R. R., 1987, A review of time domain and frequency domain component modal synthesis methods, International journal of analytical and experimental modal analysis, p. 59-72.

Craig, R. R.; Bampton, M. D. D., 1968, Coupling of substructures for dynamic analysis, AIAA Journal, p. 1313-1319.

DOI, R. M., 2011, Validação de um Modelo de Conjunto para Predição e Análise Vibroacústica de um Compressor Hermético, (Doutorado), ed. Florianópolis: [s.n.].

Fontanela, F. et al., 2016, Development of a stochastic dynamical model for hermetic compressor's components with experimental investigation, Mechanical Systems and Signal Processing.

Fulco, É. R., 2014, Modelos do Comportamento Dinâmico e Vibroacústico de Compressores Herméticos, (Doutorado), ed. Florianópolis: [s.n.].

Herting, D. N., 1985, A general purpose, multi-stage, component modal synthesis method, Finite elements in analysis and design, p. 153-164.

Kalamkarov, A. L.; Andrianov, I. V.; Danishev'kyy, V. V., 2009, Asymptotic homogenization of composite materials and structures, American Society of Mechanical Engineers, n. 3, p. 20.

Martinez, D. R. et al., 1984, Combined experimental/analytical modeling using component mode synthesis, AIAA, p. 140-152.

Millithaler, P., 2015, Dynamic behaviour of electric machine stators: modelling guidelines for efficient finite-element simulations and design specifications for noise reduction, Thesis (PhD) - l'Université de Franche-Comté, ed. Besançon: [s.n.].

Millithaler, P. et al., 2015, Structural dynamics of electric machine stators: Modelling guidelines and identification of three-dimensional equivalent material properties for multi-layered orthotropic laminates, Journal of Sound and Vibration, p. 185-205.

Mothershead, J. E.; Friswell, M. I., 1993, Model updating in structural dynamics: a survey, Journal of Sound and Vibration, p. 347-375.